Atomic Spectroscopy

Article

Chlorine Analysis in Soil Using a Transversely Excited Atmospheric (TEA) CO_2 Laser-induced Breakdown Spectroscopy Combining a Subtarget Effect and an Aqueous Extraction Method Under Helium Atmosphere

Arlin Maya Sari,[a] Birrul Walidain,[b] Muliadi Ramli,[c] Asa Miura,[d] Kazuyoshi Kurihara,[e] Marwan,[f] and Nasrullah Idris [b,*]

[a] Department of Physics Education, Faculty of Education, Universitas Malikussaleh, Aceh Utara 24355, Aceh, Indonesia

[b] Department of Physics, Faculty of Mathematics and Natural Sciences, Universitas Syiah Kuala, Darussalam, Banda Aceh 23111, Aceh, Indonesia

[c] Department of Chemistry, Faculty of Mathematics and Natural Sciences, Universitas Syiah Kuala, Darussalam, Banda Aceh, 23111, Aceh, Indonesia

[d] Department of Science and Mathematics Education, Science Education, Faculty of Education, University of Fukui 3-9-1, Bunkyo, Fukui 910-8507, Japan

[e] Department of Physics, Faculty of Education, University of Fukui 3-9-1, Bunkyo, Fukui 910-8507, Japan

[f] Department of Chemical Engineering, Faculty of Engineering, Universitas Syiah Kuala, Darussalam, Banda Aceh 23111, Indonesia

Received: *August 08, 2026;* ***Revised:*** *October 14, 2026;* ***Accepted:*** *October 16, 2026;* ***Available online:*** *October 17, 2026.*

DOI: 10.46770/AS.2026.0077s

ABSTRACT: A Transversely excited atmospheric (TEA) carbon dioxide (CO_2) laser-induced breakdown spectroscopy (LIBS) has been used to detect Cl in soil thanks to a special metal sub-target effect. The Cl sample was prepared in the form of a solution and deposited on the metal sub-target for plasma generation. For the first experiment, the Cl solution was prepared from pure chemical powder of NaCl. While for soil samples, the Cl was extracted using pure water. In this study, a CO_2 laser beam (10.6 µm, 2.5 J, 10 Hz, 200 ns) was focused on the deposited sample under the surrounding gas of helium and air at a pressure of 1 atm, respectively. It was discovered that the deposited layer on the sub-target metal (Nickel) can produce luminous plasma without damaging the metal sub-target upon the laser bombardment. Using a solution of pure chemical powder samples and a solution of standard soil mixed with pure chemical powder, emission lines from Cl can be clearly seen in the visible region, specifically Cl II 476.86 nm, Cl II 478.13 nm, Cl II 479.45 nm, Cl II 481.00 nm, Cl II 481.95 nm, Cl II 489.67 nm, Cl II 490.47 nm, and Cl II 491.77 nm. Of these, the Cl II 479.45, 481.00, and 481.95 nm triplet was detected most consistently. Strong emission intensity and low background level are two advantageous spectrochemical characteristics of the ionic emission lines. Plasma characteristics have been evaluated in terms of temperature and electron density, while the measured electron densities exceeded the minimum values required by the McWhirter criterion, although only marginally for the Hβ-based estimate, supporting the applicability of the local thermodynamic equilibrium (LTE) assumption. Calibration curves with linear tendency can be constructed for both above samples; for soil, the response is linear from 62.5 to 500 ppm (R^2 = 0.90). The detection and quantification limits of Cl in the soil, estimated from the background noise, are 35 ppm and 116 ppm, respectively. This approach has been used for the analysis of Cl contained in an actual environmental sample, namely, a tsunami-affected soil sample. Cl II emission lines were clearly detected in starch-free extracts of tsunami-affected soils collected from Banda Aceh, Indonesia, whereas in a starch-added extract of a soil from the Aceh Besar region the Cl lines were below the detection limit of the method.

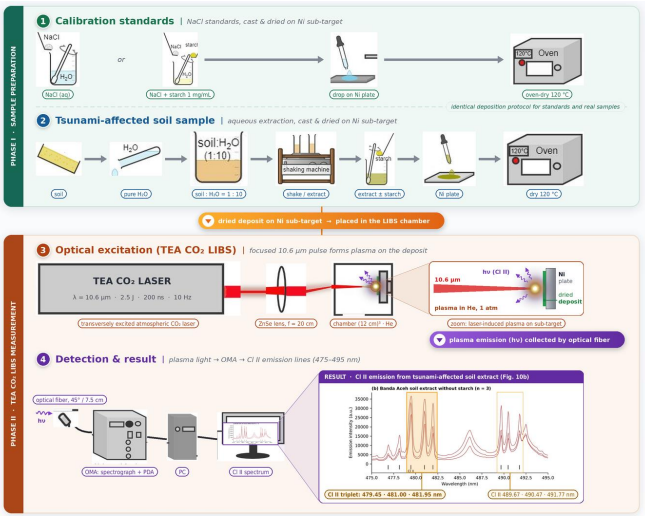

INTRODUCTION

The laser-induced breakdown spectroscopy (LIBS) technique, also known as the laser-induced plasma spectroscopy (LIPS) technique, is a rapid analysis technique for gaseous, solid, or liquid materials.[1-4] The LIBS technique has the same basic principles as other atomic emission spectroscopic techniques based on acquiring spectroscopic information from the light emitted by the atoms and ions from the plasma generated in the sample. The spectrum emission contains the characteristics of each element that can be used to identify the contents in the sample. In the LIBS technique, the plasma is formed by focusing a high-energy laser on the surface of the sample.[5,6]

The ability to detect multielements in one measurement and simple sample treatment made the LIBS technique increasingly popular for analyzing materials in various fields such as biology, geology, food, and medicine.[7-10] The LIBS technique applications for environmental monitoring, particularly soil, have been developed for pollutant contamination analysis. Several studies have successfully demonstrated the ability of the LIBS technique to monitor the excessive content of hazardous elements in the soil.[11-15]

Soil, the largest absorber on earth, contains almost all chemical elements. The Cl is a chemical element contained in the soil, which, in natural concentrations, is needed by plants. However, the excess of chlorine can trigger negative impacts such as reduced soil productivity[16] and increased absorption and accumulation of heavy metals in plants.[17] Besides, soil containing 2% wt NaCl has a high chance of experiencing premature damage due to corrosion of steel reinforcement.[18] Therefore, the information of Cl concentration in the soil is crucial.

However, the Cl analysis in soil samples using the LIBS technique needs more attention than other samples. Cl in samples such as concrete,[19-23] water,[2] and PVC[24-26] have been detected successfully using LIBS. Meanwhile, detection of Cl in soil samples has not achieved satisfactory results for monitoring applications. Soil analysis using LIBS needs sample preparation, which is not required for metal samples, to avoid the blowing-off effect. In addition, experimental parameters, such as lasers, play an important role. The Cl detection for Mars exploration has been carried out using high-power lasers (Nd:YAG) with environmental conditions matched with Mars ambients, showing high limit of detection (LOD) results[27] that are unsuitable for screening Cl in the soil in our environment. To reduce the scattering effect during the experimental process, low energy of the laser can be an option. Our previous studies found that although the soil contained very high Cl concentrations, both samples were purposely contaminated with Cl, and naturally contaminated samples (tsunami-affected soil), but Cl could not be detected in the soil samples.[28] Thus, detection of Cl using the LIBS technique faces a challenge because of its high excitation energy, and strong Cl atomic emission lines lie at the ultraviolet and infrared wavelengths. Detection of Cl in the ultraviolet range requires expensive special optical fiber, and most detectors are insensitive to infrared wavelengths. In previous research, Cl ionic emission lines in the visible range were successfully detected using TEA CO_2 LIBS on solid organic samples. A preliminary study using a metal sub-target with NaCl solution samples demonstrated up to eight Cl II emission lines in the visible range at high Cl concentration, with only a triplet of lines (Cl II 479.45, 481.00, and 481.95 nm) remaining detectable at lower concentrations.[29] The present study extends this preliminary approach by incorporating starch as a binder and applying it to real soil samples, including standard soil and tsunami-affected soil from Aceh, Indonesia.

Analysis of several pollutants in the soil was successfully carried out using the LIBS technique equipped with sub-targets.[28,30,31] The dilution method can be an option for soil sample analysis by mixing contaminated soil with water.[32,33] In addition, it was found that the CO_2 LIBS technique could be used for water content detection using the sub-target effect.[34] This study focused on detecting Cl in the soil using the CO_2 LIBS technique assisted sub-target. The extraction has been chosen as the preparation method, and measurements were made at atmospheric pressure.

EXPERIMENTAL

The targets used in this research are NaCl, CuCl, standard soil, and soil affected by the tsunami collected in Banda Aceh and Aceh Besar. All samples were prepared by the extraction method, in which the sample was dissolved into water. The sample solution was then dripped on a nickel plate, which acts as a sub-target, and was dried using an oven at a temperature of 120°C. The layer deposited on the nickel plate has been used as a target for measurement. The effect of binder material on the detection of Cl was also carried out by adding starch to the extraction solution before the drying process. The preparation process of the sample in detail has been illustrated in Fig. 1.

The Cu emission lines have been used to study the plasma characteristics generated from the samples prepared by the extraction method. Analyses were performed on the spectra of starch-added and starch-free CuCl samples, whose plasma was generated in a helium environment. Temperature and electron density were calculated according to the Boltzmann two-line method and Stark broadening, respectively, for each delay time variation. Based on the two-line Boltzmann method, the plasma temperature can be calculated using the equation

$$\frac{I_1}{I_2} = \left(\frac{g_1}{g_2}\right)\left(\frac{A_1}{A_2}\right)\left(\frac{\lambda_2}{\lambda_1}\right) exp\left(-\frac{(E_1-E_2)}{kT}\right) \quad (1)$$

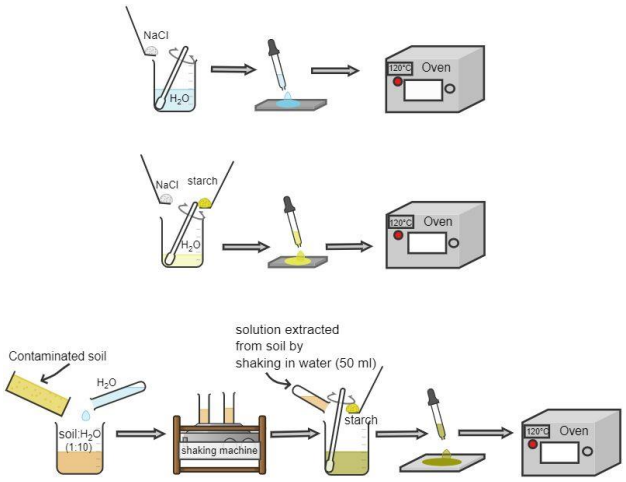

Fig. 1 Sample preparation process.

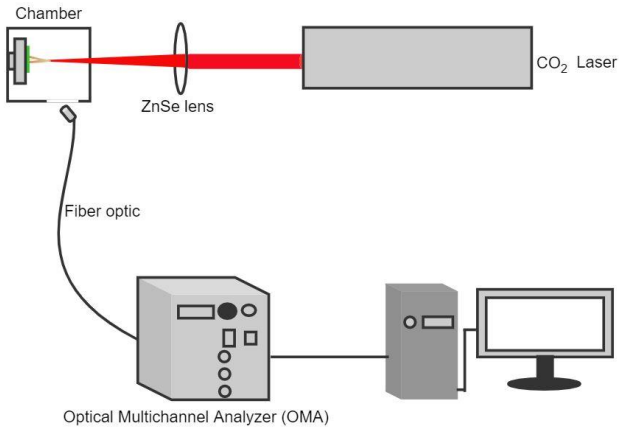

Fig. 2 LIBS experimental set-up.

Table 1. Composition of standard soil sample

Chemical compound	Percentage (%)
SiO_2	34–40
Fe_2O_3	17–23
Al_2O_3	26–32
CaO	0–3
MgO	3–7
TiO_2	0–4
Misc	0–4

subscript 1 and 2 refer to the first and second spectral lines used. I, g, A, λ, E, k, and T refer to the line intensity, the statistical weight factor for the excited states, the transition probability, the wavelength, the energy of the excited state of the two spectral lines, Boltzmann's constant, and plasma temperature, respectively. The electron density can be calculated using the FWHM of the spectral line based on the Stark broadening equation, which can be written as

$$N_e = \frac{\lambda_{FWHM}}{2.\omega}\, x10^{16} \ \ldots \qquad \ldots\ldots(2)$$

where ω is the Stark broadening parameter and Ne is the electron density.

As a cross-check, the electron density can also be estimated from the Stark width of the Hβ line (486.1 nm) using the calibration expression of Gigosos et al.[35] written as

$$N_e = 10^{17}\, x\, \left(\frac{\Delta\lambda_{FWHM(H\beta)}}{4.8}\right)^{\frac{1}{0.68116}} \ldots\ldots\ldots\ldots(3)$$

where ΔλFWHM(Hβ) is the Stark FWHM of the Hβ line (486.1 nm) in nm and Ne is the electron density in cm^{-3}.

The preparation of standard Cl-contaminated soil and tsunami-affected soil samples was carried out by mixing the soil into pure water with a ratio of 1:10. The mixture was shaken by a shaking machine for 8 hours. The 50 mL of the extracted solution was mixed with 50 mg of starch, corresponding to a starch-to-solution ratio of 1 mg/mL. For the tsunami-affected soils, extracts were measured both with and without starch; most of the starch-free spectra were recorded at a higher detector (image intensifier) gain. Then, the sample mixture was dropped on a nickel plate and dried. The sample mixture was evenly dropped onto the surface of the nickel plate, forming a layer with a uniform deposition area. The deposition procedure was performed consistently for each sample so that the distribution of the sample on the substrate surface is relatively homogeneous and does not affect the results of the quantitative measurements. The standard soil composition used in this study is presented in Table 1. The Cl concentrations in this study refer to the nominal concentrations of Cl added to the standard soil during the spiking process; the native Cl content of the standard soil was not determined.

The experimental setup from our previous study that used a CO_2 laser [26,28,31] has been adopted in this research. As shown in Fig. 2, experiments were carried out by placing the sample in a metal sample chamber (12 cm × 12 cm × 12 cm) with an air and helium environment at a pressure of 1 atm, respectively. CO_2 lasers have been used as excitation sources with pulse energies and durations of 2.5 J and 200 ns, respectively. The laser beam was focused using a ZnSe lens with a focal length of 20 cm to the surface of the material to form an optical plasma for analysis. Optical fiber guided the plasma emission to a spectrograph on an optical multichannel analyzer (OMA) system. Optical fiber was positioned at a distance of 7.5 cm from the center of plasma and 45° to the laser beam. The OMA system consists of a spectrograph and is equipped with a photodiode array detector to detect the emission spectrum. Because the detector used here is more sensitive to visible light wavelengths, the Cl analysis was focused on detecting Cl emission lines in the visible light range. Based on the database from the National Institute of Standards and Technology (NIST), the strong Cl line is in the 475–495 nm range.

RESULTS AND DISCUSSION

The sample preparation process for heterogeneous samples is crucial in measuring LIBS. For quantitative analysis accuracy, a preparation process that can make the sample more homogeneous is required. A combination of extraction methods and sub-targets has been chosen, in which the nickel plate acts as a sub-target. For each spectrum presented in this paper, the experimental conditions (laser energy, focus length, and optical device) were kept constant. The experiments were carried out in a helium environment under a pressure of 1 atm. The laser used is a CO_2 laser with a wavelength of 10.6 μm so that the possibility of overlap with the observed Cl emission line in the visible light range can be avoided. The NIST database indicates that ionic lines predominate among the strong Cl emission lines in visible light.

The first experiment was carried out on a sample of NaCl solution for testing the sub-target effect. In addition, the experiment is intended to facilitate the confirmation of the Cl emission line. NaCl powder dissolved in pure water with various concentrations of Cl. Fig. 3 demonstrates that the sample containing 1000 ppm of Cl can clearly and strongly detect the Cl ionic emission line in the visible light wavelength range. These Cl emission lines correspond to emission lines published in the NIST database and the results of previous studies on PVC samples.[25,26]

However, the emission line intensity can be affected by unstable experimental conditions. Small fluctuations in laser power during LIBS spectra recording can cause analyte line intensity changes, reducing accuracy. A calibration curve of the ratio of the analyte lines to adjacent reference lines needs to be created to achieve the accuracy of the analyte line choices in LIBS measurement. The selected reference line must be free from interference with other lines and close to the analyte line. The Hβ emission line fits these criteria, so it is chosen as the reference line. When the calibration curve in Fig. 4 is fitted to the mean intensity ratio at each concentration, the coefficient of determination (R^2) is 0.96 for the 479.45 nm line. However, when all individual replicate spectra are fitted without averaging, R^2 decreases to 0.59, with a coefficient of variation of 28–97% across concentrations, indicating that shot-to-shot fluctuations in laser power and other experimental conditions introduce substantial spectrum-to-spectrum variability even though the averaged trend remains linear. Each concentration level in Fig. 4 was measured with 2 to 5 replicate spectra, and this multiple-replicate averaging approach was applied consistently throughout the study, including for the tsunami-affected soil samples reported in the Results section.

Analysis of the NaCl solution samples showed good analytical results even without using a binder. However, the use of a binder material increases the detection sensitivity of Cl. Fig. 5 shows the comparison of the spectrum of a sample using starch as a binder and not. Both samples contained Cl with the same concentration

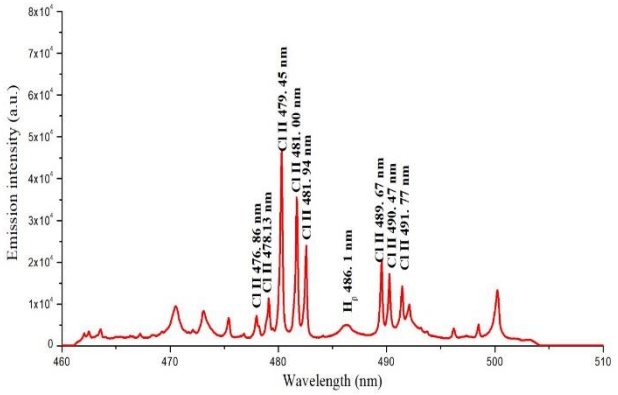

Fig. 3 LIBS spectrum emission from NaCl solution.

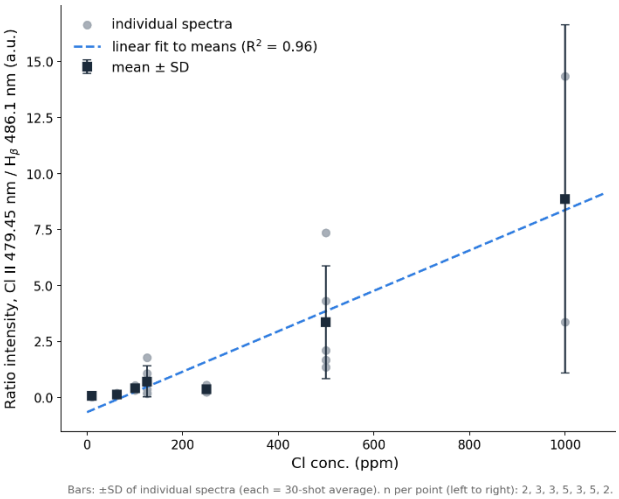

Fig. 4 Calibration curve of NaCl solution sample. Error bars: ± standard deviation of the individual spectra (n = 2–5 per concentration; each spectrum is a 30-shot average). Squares: means; dashed line: linear fit to the means.

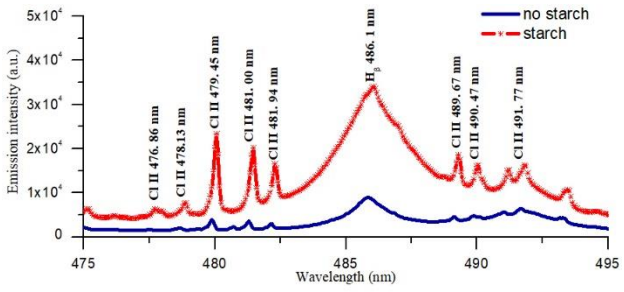

Fig. 5 Comparison of sample NaCl solution with and without the addition of binder.

of 200 ppm. Still, the intensity of Cl emission from the sample with added starch increased approximately 7.7-fold on average (range 4.3- to 9.6-fold across replicate spectra) compared to the sample without starch.

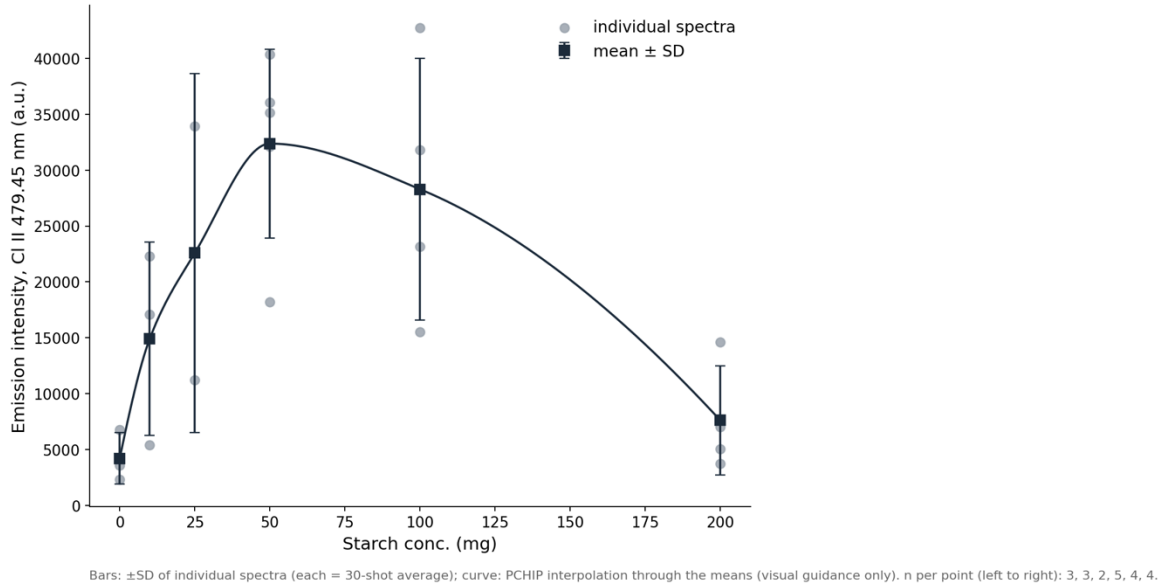

Fig. 6 Cl II 479.45 nm emission line intensity for samples with various amounts of added starch. Error bars: ± standard deviation of the individual spectra (n = 2–5 per starch level; each spectrum is a 30-shot average).

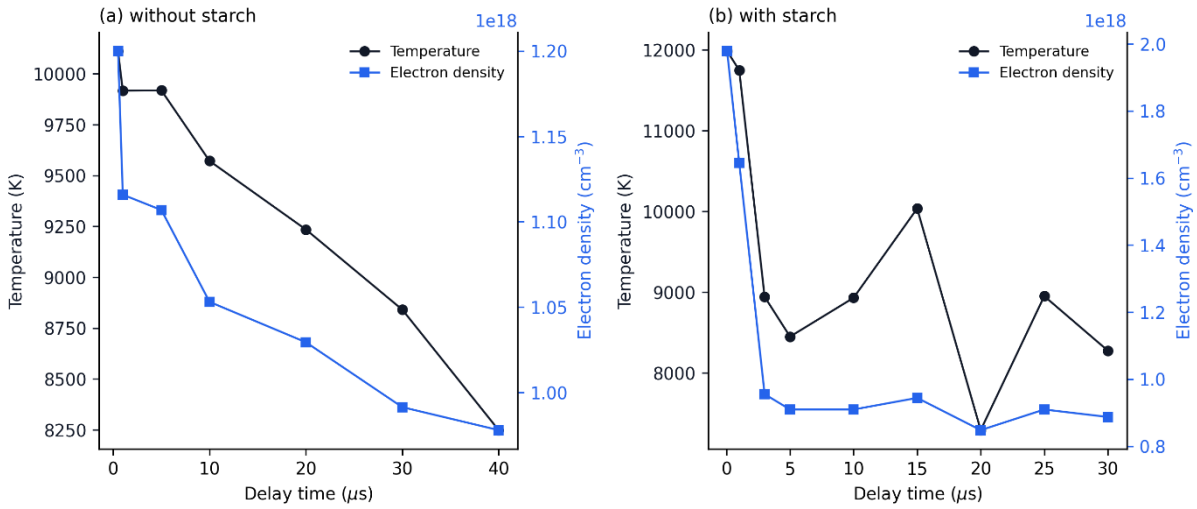

Fig. 7 Plasma temperature and electron density of CuCl sample prepared by extraction. (a) without starch; (b) with added starch.

Binder materials are used in some studies to convert the sample solution to a solid matrix.[36-39] The concentration of starch affects the detection results. Fig. 6 shows the Cl emission intensity as a function of the amount of starch added, based on all replicate spectra recorded at each condition. The mean Cl emission intensity was 32,370 ± 8,448 (n = 5) at 50 mg and 28,291 ± 11,698 (n = 4) at 100 mg of starch; this difference is not statistically significant (Welch's t-test, p = 0.58). Both 50 mg and 100 mg produced substantially higher Cl emission than the no-starch condition (mean 4,209 ± 2,282, n = 3), while 200 mg produced a lower intensity, consistent with an excessively thick binder layer reducing the laser-sample interaction. Based on these results, 50 mg of starch was selected as the working condition for subsequent measurements, since it falls within the range of maximal, statistically indistinguishable Cl enhancement while requiring less binder material than 100 mg.

The spectral emission of plasma is influenced by temperature and electron density. These two plasma characteristics as a function of time delay after the laser shot are shown in Fig. 7. Figs 7(a) and 7(b) show the plasma characteristics of the CuCl-extracted samples without starch and with added starch, respectively. The emission lines used to calculate the temperature in this study are Cu I 510.5 nm and Cu I 521.8 nm, as has also been

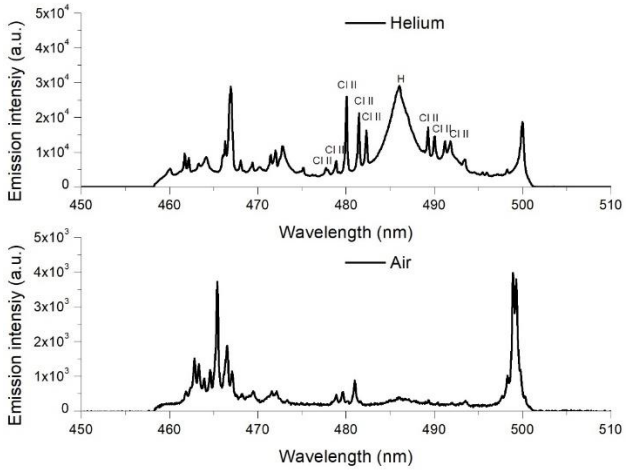

Fig. 8 Emission spectra of the Cl-spiked standard soil extract in helium and air.

used in several studies.[40,41] These two lines were selected because they are well isolated from neighboring emission lines, Cu is inherently present in the CuCl samples, and their upper levels (3.82 and 6.19 eV) span a sufficiently wide energy range, whereas the Cl II lines are relatively weak and cluster at high upper-level energies, making them less suitable for temperature estimation. The atomic parameters for calculating the plasma temperature were obtained from a database published by NIST. Meanwhile, to calculate the electron density of the Cu spectral line at a wavelength of 510.5 nm can be used.[42-44] The parameter ω needed to calculate Ne is taken from ref..[45]

The highest plasma electron density and temperature, generated from both samples, were observed at the start of the measurement. As the time delay increases, the temperature and electron density decrease due to the recombination process. Electron density decreases rapidly in the first 5 μs, then decreases slowly. The LIBS plasma is necessary to achieve local thermodynamic equilibrium (LTE) conditions to obtain accurate quantitative results. The most frequent methods used to evaluate plasmas are the Maxwell distribution and McWhirter for temperature and electron density, respectively. The kT<5 eV of temperature must be achieved for LTE conditions, while the minimum electron density to be achieved is

$$N_e \geq 1.6 \times 10^{12} T^{\frac{1}{2}} (\Delta E)^3 \ldots\ldots\ldots\ldots (4)$$

T and ΔE represent the temperature and the energy gap between the higher and the lower two states of the line used, respectively.[46]

The temperature and electron density, after spectrum analysis, both require LTE conditions. The electron density obtained from the Cu I line width is approximately three orders of magnitude above the McWhirter criterion; however, this Cu I-based estimate is likely inflated by instrumental broadening, since the observed Cu I linewidth is close to the spectrometer's resolution limit. The N_e was ~ 0.9×10^{18}–1.2×10^{18} cm^{-3} for the sample without starch and 0.8×10^{18}–1.9×10^{18} cm^{-3} for the sample with added starch. Meanwhile, calculations using McWhirter criteria are 2×10^{15}–2.3×10^{15} cm^{-3} and 1.9×10^{15}–2.3×10^{15} cm^{-3} for samples without starch and samples with added starch, respectively. Although the plasma temperature from the samples with added starch has fluctuated, the overall kT was approximately 1 eV or lower (≤ 1.03 eV). For the nonstarch condition, the Stark width of the Hβ line (486.1 nm) similarly gives Ne of 1.3×10^{16}, 2.5×10^{16}, 2.4×10^{16} and 8.5×10^{15} cm^{-3} at 0.5, 1, 5 and 20 μs (Eq. (3)), one to two orders of magnitude lower than the Cu I-based estimate above; no matching Stark dataset was recorded for the with-starch condition. Compared with the McWhirter minimum densities reported above (~2×10^{15}–2.3×10^{15} cm^{-3}), this Hβ-based Ne is only a factor of ~4–12 higher, indicating that the plasma satisfies the LTE electron-density criterion only marginally, rather than by three orders of magnitude as the Cu I-based estimate would suggest.

Soil is a material with a complex matrix and content. Thus, it is possible that the emission line of Cl interferes or overlaps with the emission lines of other elements. The extract with added starch has been applied for soil sample analysis. We recorded the spectrum from a standard soil sample in a helium and air environment, and the results were as shown in Fig. 8. The emission spectrum from standard soil extracted has not been much different from the emission spectrum from the NaCl solution sample for the helium ambient. The results show that methods of sample preparation, namely extraction, can be applied to soil samples. The plasma produced by the laser is highly influenced by the gaseous environment. The difference in the spectra observed between helium and air at atmospheric pressure can be linked to the differences in how the laser-induced plasma interacts with the surrounding gas. The composition and physical properties of the surrounding gas affect plasma shielding, energy transfer, plasma expansion, and collision processes, which in turn influence the ablation and excitation of the sample. Helium, as an inert gas, creates a different plasma environment compared to atmospheric air, which is mainly made up of nitrogen and oxygen, resulting in different plasma characteristics and emission intensities.[47]

Based on the literature, Cl can be detected under environmental conditions and the pressure of Mars. However, detecting the Cl emission line in the visible light range is difficult in the air environment.[7] In the measurement in the helium gas environment, several Cl II emission lines in the visible range were observed, though not all with equally high signal-to-noise ratio. The Cl II 479.45, 481.00, and 481.95 nm triplet was consistently detected with adequate signal-to-noise ratio (S/N ≥ 3) across replicate spectra, whereas Cl II 476.86, 478.13, 489.67, 490.47, and 491.77 nm were observed less consistently. These visible-range Cl emission

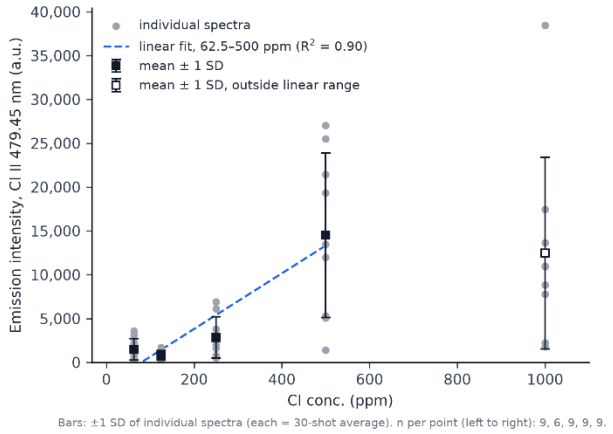

Fig. 9 Calibration curve for standard soil samples spiked with various Cl concentrations. Error bars: ± standard deviation of the individual spectra (n = 6–9 per concentration; each spectrum is a 30-shot average). Squares: means; dashed line: linear fit to the means within the linear range (62.5–500 ppm); open square: 1000 ppm, outside the linear range.

lines can still be detected at atmospheric pressure (1 atm), unlike Cl lines in the infrared range, which are more difficult to detect.[48] No emission lines from the major elements listed in the standard soil composition were found to interfere with or overlap the Cl emission lines in the measured spectra. Although some soil components may undergo dissolution or chemical transformation during the extraction process using water, the measurement results in this study did not show any observed emission lines from these components that overlapped with the selected Cl emission lines. Thus, under the experimental conditions used, no spectral interference was found that would make the Cl emission lines difficult to observe. Plasma was successfully generated from the sample layer deposited on a nickel plate using a CO_2 laser with a pulse energy of 2.5 J and a pulse duration of 200 ns. Under the experimental conditions used, no visible damage was seen on the surface of the nickel plate after the measurement process. However, since this study did not include control measurements using a nickel plate without a sample, the contribution of emissions that might come from the nickel substrate cannot be completely excluded.

The use of pulsed TEA CO_2 lasers in LIBS can produce intense plasma breakdown suitable for elemental analysis. In LIBS configurations assisted by metallic materials, TEA CO_2 lasers with a wavelength of 10.6 μm have been reported to generate plasma with high intensity through interactions between laser radiation, the metallic material, and the surrounding gas.[49] The resulting plasma can subsequently absorb laser energy through the inverse bremsstrahlung mechanism, thereby supporting the formation of plasma with a relatively large volume. The plasma absorption coefficient through this mechanism is inversely proportional to the square of the laser frequency, so CO_2 laser radiation, which has a lower frequency, can undergo stronger plasma absorption. The plasma conditions produced in this way can support the excitation and ionization processes of analyte species, thus enabling the observation of characteristic elemental emission lines.[49]

For quantitative analysis of Cl in soil, a calibration curve is required by analyzing a standard sample with the specified Cl content. The calibration curve is a graph depicting the correlation of the analyte element emission line intensity to the concentration of the standard sample. In this study, standard soil (Japan Industrial Test Powder 1 Class 7) was used. Spectrum from standard soil contaminated with Cl with various concentrations (preparation processes have been described in the experimental section) has been analyzed to create a calibration curve. We have plotted a calibration curve from five variations of Cl in a standard soil sample with a concentration range of 62.5–1000 ppm using the Cl II ionic line at 479.45 nm. The Cl intensity, as a function of Cl concentration, is shown in Fig. 9. The Cl II 479.45 nm intensity increases linearly with the Cl concentration from 62.5 to 500 ppm: a linear fit to the mean intensities gives $R^2 = 0.90$, and a lack-of-fit test against the replicate scatter does not reject the linear model ($p = 0.14$, $n = 33$ spectra). At 1000 ppm the mean intensity does not increase further, so this point lies outside the linear range and is not used for the fit; possible causes include saturation or self-absorption, which were not examined in this study. The spectrum-to-spectrum scatter is large (coefficient of variation 65–88%), partly because the plasma alternated between a helium-dominated and a sample-dominated condition, so quantitative determination within 62.5–500 ppm requires averaging several replicate spectra. Next, the 479.45 nm line will be used as an analyte line for quantitative analysis, such as calculating the limit of detection (LOD) and the limit of quantification (LOQ). LOD and LOQ can be determined using the expression

$$\mathrm{LOD} = 3 * \sigma_B/\mathrm{m} \quad (5)$$

$$\mathrm{LOQ} = 10 * \sigma_B/\mathrm{m} \quad (6)$$

The σ_B is the standard deviation of the analyte background line average, and m is the calibration curve slope. By analyzing Cl II 479.45 nm, the LOD and LOQ values in the solution sample extracted from the standard soil were 35 ppm and 116 ppm, respectively. Here, σ_B (367 counts) was taken as the standard deviation of the background signal obtained with the same peak-height procedure at a line-free wavelength in all 42 spectra, and m (31.7 counts/ppm) is the slope of the linear range. These are noise-based limits: in individual spectra, the line exceeded the background level by more than $3\sigma_B$ in only 3 of 9 spectra at 62.5 ppm and 1 of 6 at 125 ppm, compared with 6 of 9 at 250 ppm and all spectra at 500 and 1000 ppm, so reliable detection in a single spectrum requires roughly 250 ppm Cl or more.

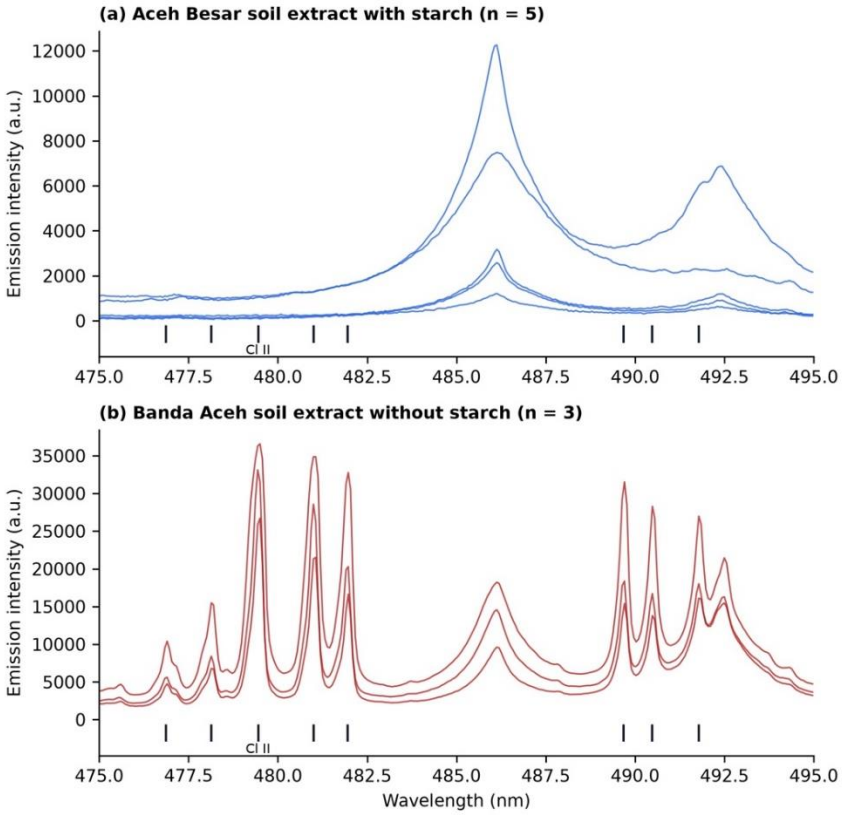

Fig. 10 LIBS spectra of tsunami-impacted soil: (a) starch-added extract of a soil from Aceh Besar; (b) starch-free extract of a soil from Banda Aceh. All replicate spectra are shown; ticks mark the Cl II lines.

Furthermore, the extraction preparation method has been applied to the analysis of Cl content in tsunami-impacted soils in Aceh. A tsunami is a natural disaster that causes a significant increase in the Cl concentration in the soil.[50] The spectrum of the analysis results is shown in Fig. 10. The tsunami-affected soil samples analyzed were taken from the Banda Aceh and Aceh Besar regions, Indonesia, which were hit by the tsunami in 2004. Previous studies reported that five years after the tsunami, Cl concentrations in tsunami-affected land exceeded 500 ppm.[50] In the analysis, we performed using the LIBS technique by recording the emission spectrum in the 475–495 nm range (strong Cl ionic emission line range). Fig. 10(a) shows the spectra of a starch-added extract of a soil from Aceh Besar, in which none of the Cl emission lines were detected. In LIBS analysis, when the analyzed line is not identified in the spectrum, it does not mean that the sample does not contain the element at all. The absence of these spectral lines in the spectrum can be affected by their concentration below the detection limit.[51] The result is supported by analysis of tsunami soil samples using other analytical techniques.[52] Based on these results, we can only conclude that the Cl content of this soil is below the detection limit of the method. The low concentration may be caused by a tsunami that occurred a long time ago, and the affected areas are tropical areas with high rainfall intensity. In contrast, Fig. 10(b) shows the spectra of a starch-free extract of a soil from Banda Aceh, in which all of the Cl II lines between 476 and 492 nm are clearly observed. Among the tsunami-affected soils measured without starch, the Cl II 479.45 nm line was detected (S/N ≥ 3) in all replicate spectra of three samples from Banda Aceh and of one sample from Aceh Besar, but not in two other samples from Aceh Besar, indicating that Cl remains detectable in some of the tsunami-affected soils. Because the starch-free spectra were recorded on a different day and mostly at a higher detector gain than the starch-added spectra, the two conditions cannot be compared directly, and the Cl concentrations of these samples were not quantified with the calibration in Fig. 9, which was obtained from starch-added extracts.

CONCLUSIONS

A novel method that employs TEA CO_2 Laser-Induced Breakdown Spectroscopy (LIBS) to detect chlorine (Cl) in soil, leveraging the distinctive metal sub-target effect has been developed. This study described a soil sample preparation method

for LIBS measurement dedicated to qualitative and quantitative Cl analysis. The sample has been prepared by extracting the soil sample. For the first measurement, plasma has been generated from the NaCl solution sample. The result shows that adding starch as a binder can increase the sensitivity of Cl detection in NaCl solution samples. In the helium ambient at atmospheric pressure, the Cl emission line could be detected via ionic line in the visible range, namely Cl II 476.86 nm, Cl II 478.13 nm, Cl II 479.45 nm, Cl II 481.00 nm, Cl II 481.95 nm, Cl II 489.67 nm, Cl II 490.47 nm, and Cl II 491.77 nm, of which the Cl II 479.45, 481.00, and 481.95 nm triplet was detected most consistently. Calibration curve has been made from a standard soil sample using the Cl II 479.45 nm line and found a linear response from 62.5 to 500 ppm, with noise-based LOD and LOQ of 35 ppm and 116 ppm, respectively. The characteristics of plasma generated from an extracted sample, namely temperature and electron density, were used to check the McWhirter criterion for LTE. Based on this research, the preparation method was applied to Cl detection in tsunami-impacted soils in Banda Aceh and Aceh Besar, Indonesia. Cl was clearly detected in starch-free extracts of the Banda Aceh soils, whereas in the starch-added extract of an Aceh Besar soil it was below the detection limit of the method. Future work may explore enhancing the Cl signal by applying an external electric field to the plasma and by measuring the Cl I 837.59 nm line, as suggested by Ahmed et al.[41]

AUTHOR INFORMATION

Nasrullah Idris received his D. Eng. in Fiber Amenity Engineering from the University of Fukui, Japan, followed by Japan Society for the Promotion of Science (JSPS) and Training and Research in Italian Laboratories (TRIL) postdoctoral fellowships focusing on laser-induced breakdown spectroscopy (LIBS). Currently he is a Professor at Department of Physics, Universitas Syiah Kuala, Indonesia. He has authored and co-authored over 120 scientific papers. His research spans the mechanics and applications of LIBS for spectrochemical analysis, including nuclear zircaloy tube hydrogen analysis, building material inspection, and soil pollution monitoring. His recent work focuses on the geochemical analysis of tsunami-impacted, coastal, and volcanic soils, as well as organic food authentication, including incorporating chemometrics and artificial intelligence (AI) for advanced spectral analysis.

Corresponding Authors

*** N. Idris**

Email address: nasrullah.idris@usk.ac.id

Notes

The authors declare no competing financial interest.

ACKNOWLEDGMENTS

The USK Leading Research Program for Doctoral Acceleration (Program Riset Unggulan USK Percepatan Doktor, PRUUPD) 2020, with contract number 318/UN11.2.1/PT.01.02/PNBP/2020, provided financial support to the authors (N. I., M. R., A. M. S., and M.) via Universitas Syiah Kuala (USK), Aceh, Indonesia on March 26, 2020. The University of Fukui, Fukui, Japan, provided partial financial support for this research in 2017 and 2018, for which the authors (N. I., M. R., and K. K.) are grateful.

REFERENCES

1. M. Tran, B. W. Smith, D. Hahn, and J. D. Winefordner, *Appl. Spectrosc.*, 2001, **55**, 1455–1461. https://doi.org/10.1366/0003702011953865
2. S. Ma, Y. Tang, S. Zhang, Y. Ma, Z. Sheng, Z. Wang, L. Guo, J. Yao, and Y. Lu, *Talanta*, 2020, **214**, 120849. https://doi.org/10.1016/j.talanta.2020.120849
3. N. Idris, K. Lahna, T. N. Usmawanda, Herman, M. Ramli, R. Hedwig, A. M. Marpaung, and K. H. Kurniawan, *J. Phys.: Conf. Ser.*, 2018, **1011**, 012057. https://doi.org/10.1088/1742-6596/1011/1/012057
4. F. Bencherif, S. A. Beldjilali, T. Baba-Hamed, and A. Belasri, *Optik*, 2020, **224**, 165573. https://doi.org/10.1016/j.ijleo.2020.165573
5. F. C. DeLucia, A. C. Samuels, R. S. Harmon, R. A. Walters, K. L. McNesby, A. LaPointe, R. J. Winkel, and A. W. Miziolek, *IEEE Sens. J.*, 2005, **5**, 681–689. https://doi.org/10.1109/JSEN.2005.848151
6. J. P. Singh, J. R. Almirall, M. Sabsabi, and A. W. Miziolek, *Anal. Bioanal. Chem.*, 2011, **400**, 3191-3192. https://doi.org/10.1007/s00216-011-5073-5
7. B. Sallé, J. L. Lacour, E. Vors, P. Fichet, S. Maurice, D. A. Cremers, and R. C. Wiens, *Spectrochim. Acta B*, 2004, **59**, 1413–1422. https://doi.org/10.1016/j.sab.2004.06.006
8. H. Wiggenhauser, D. Schaurich, and G. Wilsch, *NDT & E Int.*, 1998, **31**, 307–313. https://doi.org/10.1016/S0963-8695(98)00008-5
9. C.-T. Chen, D. Banaru, T. Sarnet, and J. Hermann, *Spectrochim. Acta B*, 2018, **150**, 77–85. https://doi.org/10.1016/j.sab.2018.10.011
10. R. K. Aldakheel, M. A. Gondal, M. M. Nasr, M. A. Almessiere, and N. Idris, *Talanta*, 2020, **217**, 121062. https://doi.org/10.1016/j.talanta.2020.121062
11. S. Pandhija and A. K. Rai, *Environ. Monit. Assess.*, 2009, **148**, 437–447. https://doi.org/10.1007/s10661-008-0173-1
12. M. Akhtar, A. Jabbar, S. Mehmood, N. Ahmed, R. Ahmed, and M. A. Baig, *Spectrochim. Acta B*, 2018, **148**, 143–151. https://doi.org/10.1016/j.sab.2018.06.016
13. N. Idris, K. Kagawa, F. Sakan, K. Tsuyuki, and S. Miura, *Appl. Spectrosc.*, 2007, **61**, 1344–1351. https://doi.org/10.1366/000370207783292181
14. M. Ramli, A. Khumaeni, K. H. Kurniawan, M. O. Tjia, and K. Kagawa, *Spectrochim. Acta B*, 2017, **132**, 8–12. https://doi.org/10.1016/j.sab.2017.03.017

15. N. Idris, M. A. Gondal, K. Lahna, M. Ramli, A. M. Sari, R. K. AlDakheel, R. Mitaphonna, M. A. Dastageer, K. Kurihara, K. H. Kurniawan, and M. A. Almessiere, *Arab. J. Chem.*, 2022, **15**, 103847. https://doi.org/10.1016/j.arabjc.2022.103847
16. D. Tilman, K. G. Cassman, P. A. Matson, R. Naylor, and S. Polasky, *Nature*, 2002, **418**, 671–677. https://doi.org/10.1038/nature01014
17. H. Li, Z. Li, M. A. Khaliq, T. Xie, Y. Chen, and G. Wang, *Chemosphere*, 2019, **235**, 1172–1179. https://doi.org/10.1016/j.chemosphere.2019.06.203
18. M. A. Baltazar-Zamora, J. M. Mendoza-Rangel, R. Croche, C. Gaona-Tiburcio, C. Hernández, L. López, F. Olguín, and F. Almeraya-Calderón, *Front. Mater.*, 2019, **6**, 00257. https://doi.org/10.3389/fmats.2019.00257
19. G. Asimellis, A. Giannoudakos, and M. Kompitsas, *Spectrochim. Acta B*, 2006, **61**, 1270–1278. https://doi.org/10.1016/j.sab.2006.10.014
20. C. D. Gehlen, E. Wiens, R. Noll, G. Wilsch, and K. Reichling, *Spectrochim. Acta B*, 2009, **64**, 1135–1140. https://doi.org/10.1016/j.sab.2009.07.021
21. T. A. Labutin, A. M. Popov, S. N. Raikov, S. M. Zaytsev, N. A. Labutina, and N. B. Zorov, *J. Appl. Spectrosc.*, 2013, **80**, 315–318. https://doi.org/10.1007/s10812-013-9766-8
22. F. Weritz, D. Schaurich, and G. Wilsch, *Spectrochim. Acta B*, 2007, **62**, 1504–1511. https://doi.org/10.1016/j.sab.2007.10.017
23. W. Zhang, R. Zhou, P. Yang, K. Liu, J. Yan, P. Gao, Z. Tang, X. Li, Y. Lu, and X. Zeng, *Talanta*, 2019, **198**, 93–96. https://doi.org/10.1016/j.talanta.2019.01.102
24. N. Idris, T. Kobayashi, M. M. Sullyanti, H. Kurniawan, T. J. Lie, K. Kagawa, and Y. I. Lee, *J. Korean Phys. Soc.*, 2005, **47**, 256–262. https://www.academia.edu/27255978
25. A. M. Sari, K. Lahna, N. Idris, M. Ramli, and K. Kurihara, *Earth Environ. Sci.*, 2019, **364**, 012017. https://doi.org/10.1088/1755-1315/364/1/012017
26. A. M. Sari, K. Lahna, M. Ramli, K. Kurihara, and N. Idris, *IOP Conf. Ser.: Mater. Sci. Eng.*, 2020, **796**, 012030. https://doi.org/10.1088/1757-899X/796/1/012030
27. L. Radziemski, D. A. Cremers, K. Benelli, C. Khoo, and R. D. Harris, *Spectrochim. Acta B*, 2005, **60**, 237–248. https://doi.org/10.1016/j.sab.2004.12.007
28. A. M. Sari, M. Ramli, K. Kurihara, and N. Idris, *J. Phys.: Conf. Ser.*, 2018, **1116**, 032028. https://doi.org/10.1088/1742-6596/1116/3/032028
29. A. M. Sari, K. Lahna, M. Ramli, A. Miura, K. Kurihara, Marwan, and N. Idris, *J. Phys.: Conf. Ser.*, 2021, **1816**, 012034. https://doi.org/10.1088/1742-6596/1816/1/012034
30. N. Idris, M. Ramli, and K. Kurihara, in *2016 International Seminar on Sensors, Instrumentation, Measurement and Metrology (ISSIMM)*, Malang, IEEE, 2016, pp. 79–83. https://doi.org/10.1109/ISSIMM.2016.7803727
31. N. Idris, A. M. Sari, M. Ramli, and K. Kurihara, *J. Phys.: Conf. Ser.*, 2018, **1120**, 012019. https://doi.org/10.1088/1742-6596/1120/1/012019
32. S. C. Jantzi, V. Motto-Ros, F. Trichard, Y. Markushin, N. Melikechi, and A. De Giacomo, *Spectrochim. Acta B*, 2016, **115**, 52–63. https://doi.org/10.1016/j.sab.2015.11.002
33. N. Yang, N. S. Eash, J. Lee, M. Z. Martin, Y. S. Zhang, F. R. Walker, and J. E. Yang, *Soil Sci.*, 2010, **175**, 447–452. https://doi.org/10.1097/SS.0b013e3181f516ea
34. Y. I. Lee, N. Idris, K. H. Kurniawan, T. J. Lie, K. Tsuyuki, S. Miura, and K. Kagawa, *Curr. Appl. Phys.*, 2007, **7**, 540–546. https://doi.org/10.1016/j.cap.2006.11.035
35. M. A. Gigosos, M. A. Gonzalez, and V. Cardenoso, *Spectrochim. Acta B*, 2003, **58**, 1489–1504. https://doi.org/10.1016/S0584-8547(03)00097-1
36. S. Millar, C. Gottlieb, T. Günther, N. Sankat, G. Wilsch, and S. Kruschwitz, *Spectrochim. Acta B*, 2018, **147**, 1–8. https://doi.org/10.1016/j.sab.2018.05.015
37. M. A. Gondal, T. Hussain, Z. H. Yamani, and M. A. Baig, *Talanta*, 2007, **72**, 642–649. https://doi.org/10.1016/j.talanta.2006.11.039
38. J. O. Cáceres, J. Tornero López, H. H. Telle, and A. González Ureña, *Spectrochim. Acta B*, 2001, **56**, 831–838. https://doi.org/10.1016/S0584-8547(01)00173-2
39. D. M. Díaz Pace, C. A. D'Angelo, D. Bertuccelli, and G. Bertuccelli, *Spectrochim. Acta B*, 2006, **61**, 929–933. https://doi.org/10.1016/j.sab.2006.07.003
40. Y. Sasaki and K. Wagatsuma, *Anal. Sci.*, 2009, **25**, 481–485. https://doi.org/10.2116/analsci.25.481
41. R. Ahmed, A. Jabbar, M. Akhtar, Z. A. Umar, and M. A. Baig, *Plasma Chem. Plasma Process.*, 2020, **40**, 809–818. https://doi.org/10.1007/s11090-020-10072-4
42. J. Hermann, A. Lorusso, A. Perrone, F. Strafella, C. Dutouquet, and B. Torralba, *Phys. Rev. E*, 2015, **92**, 053103. https://doi.org/10.1103/PhysRevE.92.053103
43. E. Mal, R. Junjuri, M. K. Gundawar, and A. Khare, *J. Anal. At. Spectrom.*, 2019, **34**, 319–330. https://doi.org/10.1039/c8ja00415c
44. R. Junjuri, S. A. Rashkovskiy, and M. K. Gundawar, *Phys. Plasmas*, 2019, **26**, 123302. https://doi.org/10.1063/1.5118289
45. B. Zmerli, N. Ben Nessib, M. S. Dimitrijević, and S. Sahal-Bréchot, *Phys. Scr.*, 2010, **82**, 055301. https://doi.org/10.1088/0031-8949/82/05/055301
46. S. Zhang, X. Wang, M. He, Y. Jiang, B. Zhang, W. Hang, and B. Huang, *Spectrochim. Acta B*, 2014, **97**, 13–33. https://doi.org/10.1016/j.sab.2014.04.009
47. A. Effenberger and J. Scott, *Sensors*, 2010, **10**, 4907–4925. https://doi.org/10.3390/s100504907
48. G. Asimellis, S. Hamilton, A. Giannoudakos, and M. Kompitsas, *Spectrochim. Acta B*, 2005, **60**, 1132–1139. https://doi.org/10.1016/j.sab.2005.05.035
49. A. Khumaeni, W. S. Budi, K. H. Kurniawan, and K. Kurihara, *J. King Saud Univ. Sci.*, 2022, **34**, 101901. https://doi.org/10.1016/j.jksus.2022.101901
50. S. K. Chaerun, W. B. Whitman, S. J. Wirth, and R. H. Ellerbrock, in *26th Annual Meetings of the American Society of Mining and Reclamation and 11th Billings Land Reclamation Symposium*, 2009, vol. 1, pp. 210–226. https://doi.org/10.21000/jasmr09010210
51. J. El Haddad, L. Canioni, and B. Bousquet, *Spectrochim. Acta B*, 2014, **101**, 171–182. https://doi.org/10.1016/j.sab.2014.08.039
52. R. Mitaphonna, M. Ramli, N. Ismail, and N. Idris, *Philipp. J. Sci.*, 2023, **152**, 485–499. https://philjournalsci.dost.gov.ph/evaluation-of-geochemical-signature-in-soil-sampled-from-a-2004-indian-ocean-tsunami-stricken-region-in-aceh-province-located-in-the-western-part-of-indonesia-using-scanning-electron-microscopy/